6-2003

Three-Dimensional Model of Modern Channel Bend Deposits

M. Bayani Cardenas
New Mexico Institute of Mining and Technology, cardenas@jsg.utexas.edu

Vitaly A. Zlotnik
University of Nebraska-Lincoln, vzlotnik1@unl.edu

Three-dimensional model of modern channel bend deposits

M. Bayani Cardenas[1] and Vitaly A. Zlotnik

Department of Geosciences, University of Nebraska at Lincoln, Lincoln, Nebraska, USA

Received 15 April 2002; revised 22 July 2002; accepted 13 March 2003; published 4 June 2003.

[1] We present a three-dimensional model of heterogeneous modern channel bend deposits developed through purely structure-imitating interpolation (kriging) of hydraulic properties. This model, augmented with ground-penetrating radar data and directional variograms, agrees with detailed observations in similar modern environments and leads to a process-based interpretation of the presented hydraulic conductivity structure. Integration of all available information permitted delineation and characterization of the modern streambed as a distinct hydrostratigraphic unit without coring or outcrop studies. Our results imply that the modern streambed is commonly oversimplified in available analytical and numerical models of groundwater-surface water interactions where it is assumed to be homogeneous and isotropic and characterized by a constant width and thickness. This three-dimensional approach that integrates concepts and principles developed in sedimentology, hydrogeology, geophysics, and geostatistics has potential implications on model development of stream-aquifer systems. *INDEX TERMS:* 1829 Hydrology: Groundwater hydrology; 1824 Hydrology: Geomorphology (1625); 1815 Hydrology: Erosion and sedimentation; 5114 Physical Properties of Rocks: Permeability and porosity; 1894 Hydrology: Instruments and techniques; *KEYWORDS:* hydraulic conductivity, bend deposits, streambed conductance, hyporheic zone, heterogeneity, ground-penetrating radar

Citation: Cardenas, M. B., and V. A. Zlotnik, Three-dimensional model of modern channel bend deposits, *Water Resour. Res.*, *39*(6), 1141, doi:10.1029/2002WR001383, 2003.

1. Introduction

[2] The spatial variability of hydraulic conductivity (K) or permeability determines groundwater flow and solute transport at various spatial and timescales [*Gelhar et al.*, 1992; *Gelhar*, 1993]. Thus one of the most basic pursuits of modern hydrogeology is the determination of the heterogeneity of porous media [*Webb and Davis*, 1998].

[3] The generation of maps of heterogeneous aquifers has been categorized into three approaches [*Koltermann and Gorelick*, 1996]: structure-imitating, process-imitating, and descriptive. Structure-imitating methods include geostatistical interpolation techniques and sedimentation geometry-matching approaches. Process-imitating techniques generate images via solving governing mass and momentum balance equations of fluid and sediment flow and transport. Descriptive approaches involve delineation of domains based on direct observations and genetic conceptual models (facies).

[4] These approaches have various advantages and limitations [*Koltermann and Gorelick*, 1996]. Structure-imitating models commonly result in unrealistic images. Process-based models generate models that are more physically plausible, although it is difficult to condition them to actual data. Descriptive methods are able to include physical insight but do not generate results with sufficient accuracy. It is therefore apparent that integration of these techniques will allow effective and more realistic representation of spatial variability of hydraulic properties of aquifers [*Webb and Davis*, 1998].

[5] In this paper, we present a three-dimensional (3D) model of the modern streambed of a meander bend that is generated exclusively through a structure-imitating method-3D kriging. Our realization is based on extensive direct small-scale hydraulic tests that cover most of the study domain. These K estimates are augmented with data from cores and ground-penetrating radar (GPR) profiles. This data set allowed us to examine the 3D geostatistical properties (variograms) of the tested media. Additionally, we are able to favorably compare our observations to results from detailed investigations of modern surface deposits in similar settings [*Bridge*, 1977]. Such studies directly link processes and products and allow us to interpret our results in a process-oriented framework. Through this integrative interpretive approach of data of different nature (hydraulically based, core-based, and geophysically based), we are able to separate the streambed from its adjacent hydrostratigraphic units. In addition to identification of the streambed as a distinct hydrofacies, we also present its effective hydraulic parameters derived through various upscaling methods.

[6] In a practical sense, delineation and characterization of the modern streambed has significant implications on groundwater-surface water interactions [*Sophocleous et al.*, 1995; *Zlotnik and Huang*, 1999; *Hunt et al.*, 2001; *Butler et al.*, 2001]. Our research was conducted within this context although most investigations of heterogeneity are commonly related to contaminant transport and remediation problems. A standing issue in water-resource management is how streams interact with groundwater. Unfortunately, most studies that address this problem have considered the

[1]Now at Department of Earth and Environmental Science, New Mexico Institute of Mining and Technology, Socorro, New Mexico, USA.

0043-1397/03/2002WR001383$09.00

streambed as an entity of well-defined geometric and effective hydraulic properties. Our results show that the modern streambed (sometimes referred to as the "hyporheic zone" in special cases [*Woessner*, 2000]) at our study site, which is part of a fluvial system typical of the High Plains of the Midwestern United States, is far from its common representation in both numerical and analytical models.

[7] Considering the important role of the streambed in various natural processes, the focus of this paper is the development of a realistic 3D model of the modern streambed from analyses of spatial variations of hydraulic properties used as proxies of architectural elements. The developed model should allow us to confidently separate it from its surrounding units. Although we chose to represent the 3D K field of the streambed as a continuum (which is inherent in the kriging process) and not through simulating discrete units, we are able to show that our realization is realistic by comparing it with deposits in similar modern environments. We present a case where a purely structure-imitating model agrees with well-documented modern surface deposits, which allows us to confidently delineate the streambed. This approach of characterizing modern streambed deposits along meander bends, whose depositional processes are readily observed, has numerous implications not only in studies related to realistic image generation of porous media but also in existing hydrogeologic models that include the streambed.

2. Previous Work and Goals of the Study

[8] Different combinations of interpolation tools have been effected on fluvial channel deposits. The structure of meander deposits at the submeter scale has been simulated in the form of a "numerical aquifer" developed via a hierarchical geometric model [*Scheibe and Freyberg*, 1995]. Simulation of point bar deposits at the meter scale that consider cross bedding has also been implemented [*Bierkens and Weerts*, 1994]. Likewise, *Webb and Anderson* [1996] simulated braided-stream deposits via a random walk process.

[9] Process-based simulations have modeled deposits from pore-scale to basin-scale and from seconds to hundred-thousand year time domains. For example, *Bridge* [1977, 1992] simulated the surficial distribution of grains along a meander during high-flow conditions. The 3D simulation of meandering stream deposits has not been extensive though due to the complexity of the processes involved, although this is a subject of ongoing investigation [*Sun et al.*, 2001].

[10] In hydrogeologic models, the streambed has been investigated using different procedures. The few studies that have been undertaken involved different approaches: numerical modeling, pumping tests, laboratory measurements, analytical calculations and combinations of the above methods [*Calver*, 2001]. However, direct hydraulic measurements within active channels are still rare.

[11] In the past decade, river ecologists focused their attention on the interface, the "hyporheic zone", where exchanges between groundwater and stream water occur [*Palmer*, 1993; *Bencala*, 1993; *Woessner*, 2000]. The significance of the streambed or "clogging layer" in streamflow depletion when wells are located adjacent to rivers has been widely recognized in hydrogeology and water resource management [*Sophocleous et al.*, 1995; *Zlotnik et al.*, 1999; *Zlotnik and Huang*, 1999; *Hunt et al.*, 2001; *Butler et al.*, 2001; *Calver*, 2001; *Kollet and Zlotnik*, 2003]. Both hydrogeologists and ecologists advocate better delineation of the heterogeneity and extent of the streambed in order to better understand its effects on channel-scale processes. However, the extent and nature of a streambed remain poorly defined due to the inherent difficulties in actual field measurements. Owing to these obstacles [*Palmer*, 1993; *Harvey et al.*, 1996; *Woessner*, 2000; *Calver*, 2001], representation of the streambed as a layer of uniform thickness and lower K is prevalent in applied hydrogeology [*McDonald and Harbaugh*, 1984].

[12] *Palmer* [1993] distinguishes hydrologic and geomorphic approaches in the delineation of the streambed. The hydrologic approach entails the direct delineation of the flow field of the systems involved- usually through tracer tests (both simulated and actual) and measurements of local hydraulic gradients [*Harvey et al.*, 1996]. Most of these studies investigated the lateral, and sometimes vertical, extent of the hyporheic zone.

[13] The geomorphic approach focuses on the geometry and composition of the hyporheic substrate [*Palmer*, 1993]. This procedure is normally applied in alluvial valleys where the surface of the underlying bedrock is assumed to be the maximum extent of the hyporheic zone. This method is complicated when modern streambed sediments overlie similar older alluvial deposits. We present an integration of the geomorphic and hydrologic methods.

[14] The main goal of the study is to delineate the modern streambed from its adjacent hydrostratigraphic units. This is achieved through three objectives: (1) quantify the heterogeneity of the streambed through small-scale hydraulic tests on a 3D grid and through geostatistical analysis and data visualization, (2) map bounding (scour) surfaces using GPR, and (3) and analyze the results in a process-based sedimentologic context.

3. Prairie Creek Test Site

[15] The test site (in central Nebraska, USA) is located along a meander bend of the Prairie Creek (Figure 1). The site hosts a network of clustered observation wells, two stream gauges, and a high-capacity pumping well situated about 50 m from the channel that are used for assessment of stream depletion [*Kollet and Zlotnik*, 2003]. The drainage area of the Prairie Creek is about 250 km^2, typical for small streams in the Great Plains region. Its watershed is bounded by the Loup River to the north and the Platte River, which it eventually joins, to the south. The discharge at the stream gauging station upstream from the site varies from dry conditions during summer droughts to about 50 m^3/s during spring floods.

[16] The principal geologic units of the area include Cretaceous bedrock that consists mostly of shales, semi-consolidated to unconsolidated Tertiary fluvial sediments, and Quaternary alluvium [*Sniegocki*, 1955]. Of these, the most productive aquifer is the Tertiary Ogallala Formation that extends northward to South Dakota, and southward to Texas. However, most of the wells in the vicinity of the site are screened in the upper unconfined aquifer that consists of Quaternary sands and gravels intercalated with minor silt and clay layers of fluvial and eolian origin. Most of the

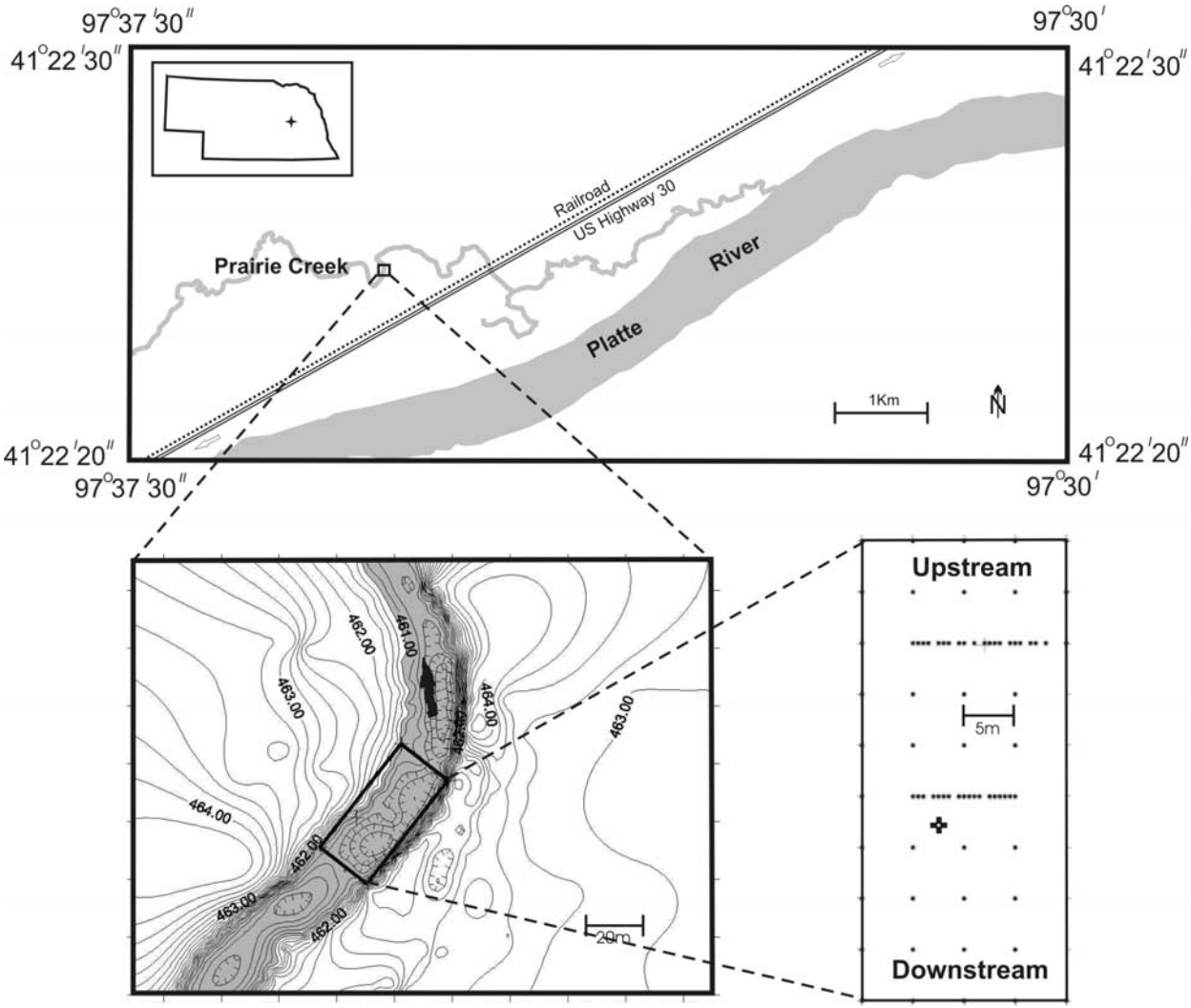

Figure 1. Topographic map of the Prairie Creek test site, Nebraska. Solid circles denote location of injection tests in blown-up grid. The open circle indicates location of coupled injection tests and slug tests, and the four surrounding squares are core locations.

Pleistocene sands and gravels in the area are associated with the Platte River. This unconfined aquifer is about 17 m thick at the test site and is underlain by a continuous clay layer.

4. Methodology

4.1. Estimation of Local Hydraulic Conductivity

[17] There are several techniques available for in situ estimation of K of the streambed [*Landon et al.*, 2001]. To derive a 3D K distribution though, multilevel slug tests offer a suitable method that will allow estimation of K in a 3D field [*Zlotnik and McGuire*, 1998; *Rus et al.*, 2001]. This technique will see more application in the future with the advent of direct-push technology [e.g., *Hinsby et al.*, 1992]. However, few data on K of the modern streambed derived through slug testing have been published [*Calver*, 2001]. The exceptions are those of *Duwelius* [1996], *Springer et al.* [1999], and *Rus et al.* [2001].

[18] Three techniques to estimate K of streambed materials were first compared in preliminary experiments. They included two small-scale in situ hydraulic tests and grain-size analysis of cores. Multilevel constant-head injection tests (CHIT) and multilevel slug tests were conducted on the same intervals of a single test hole. This was accomplished by driving a screened drive-point (with 0.2 mm slot size, 4.3 cm outer diameter, 2.5 cm inner diameter and a 20 cm screen length) at successive intervals using a post-driver.

[19] The setup of our slug tests (Figure 2) is similar to that of *Rus et al.* [2001]. Water level in the minipiezometer was lowered by using a pneumatic device. Three different head displacements, y_o, were used at each point in order to verify test reproducibility, occurrence of development of the area adjacent the screen, and nonlinear effects [*Zurbuchen et al.*, 2002]. The wells were purged before each set of tests. All the acquired slug test responses were overdamped and were analyzed using the *Bouwer and Rice* [1976] method. The K estimates ranged from 3 m/d to 37 m/d. Different head displacements gave similar values for K, supporting the reproducibility of this method.

[20] Slug tests at each point were followed by CHIT's. Water from a graduated carboy was injected into the piezometer (Figure 2), and constant-head increase y_o and

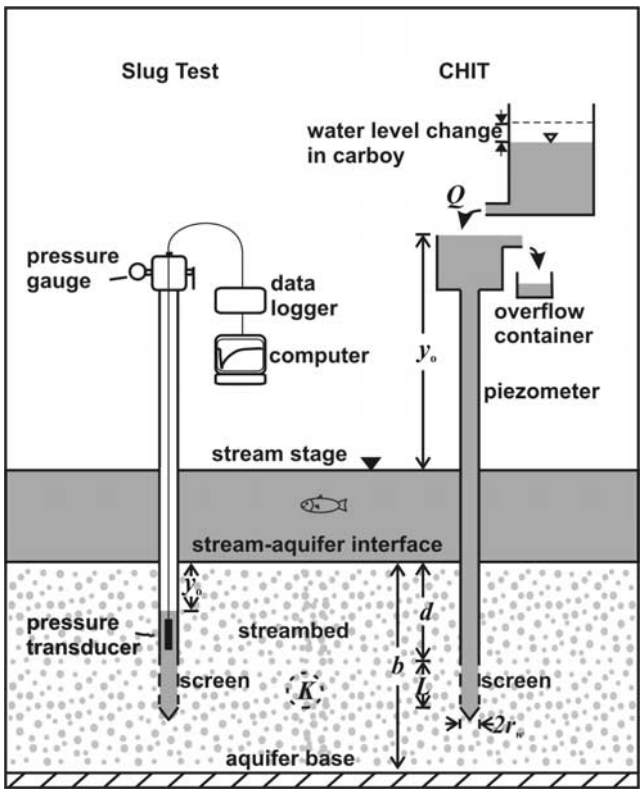

Figure 2. Schematic representation of slug test and CHIT.

discharge Q were measured after steady state was achieved. K was estimated using modified Thiem equation [see *Zlotnik*, 1994, equation 3]:

$$K = \frac{Q}{2\pi L P y_o} \tag{1}$$

where P is shape factor and L is screen length. Conditions of our test correspond exactly to the *Bouwer and Rice* [1976] shape factor [see *Zlotnik*, 1994, equation 5]:

$$P = \frac{1.1}{\ln((d+L)/r_w)} + \frac{A + B\ln[b-(d+L)/r_w]}{L/r_w} \tag{2}$$

where r_w is the radius of the well, b is the aquifer saturated thickness, d is the distance to the top of the screen from the water table, and A and B are dimensionless coefficients after *Bouwer and Rice* [1976]. A and B can be approximated with polynomial functions (see equations by Van Rooy as given in the work by *Butler* [1998]). Following *Bouwer and Rice* [1976], it was assumed that the aquifer is isotropic at the scale of the CHIT.

[21] Similar to the slug tests, CHIT's also showed K estimates, varying from 2 m/d to 30 m/d, which are reproducible (Figure 3). We repeated three tests at each interval using the same head increase. Additional experiments showed that head increase is proportional to discharge and that nonlinear effects are absent.

[22] Four cores, each 0.5 m away from the test hole (Figure 1), were extracted through vibracoring. The cores were divided into 10 cm sections that were then sieved into 15 grain-size intervals. K values were derived from the distributions through the program MVASKF [*Vukovic and Soro*, 1992] that uses 10 different empirical equations. Not surprisingly, the different formulas gave a range of values.

[23] The MVASKF code uses a modified form of the Hazen equation. We also applied its widely used classic form:

$$K = Cd_{10}^2 \tag{3}$$

where C ranges from 100–150 for loose sand, d_{10} is expressed in cm, and K in cm/s. This resulted in K values that are higher than those acquired through hydraulic testing (Figure 3).

[24] Amongst the empirical equations that we used, the Terzaghi formula agrees well with data from both hydraulic tests (Figure 3). This formula in dimensionally homogeneous form is as follows:

$$K = \frac{g}{v} C_T \left(\frac{n - 0.13}{\sqrt{[3]1-n}} \right)^2 d_{10}^2 \tag{4}$$

where g is gravitational acceleration, v is kinematic viscosity, d_{10} is the effective grain size, and C_T is a dimensionless empirical coefficient depending on grain shape. We use C_T = 0.0084, which is the middle of commonly suggested range of values for sand. The values for porosity n were computed using the following empirical equation [*Vukovic and Soro*, 1992] that utilizes uniformity coefficient $\eta = d_{60}/d_{10}$:

$$n = 0.255(1 + 0.83\ \eta) \tag{5}$$

[25] The mean coefficients of variation of the K estimates (from repeated tests at each test interval) are below 0.05 for both CHIT's and slug tests. A paired sample t-test for the two techniques showed that the hypothesis that the mean difference between the two tests is zero could not be rejected at a 5% level of significance [*Dowdy and Wearden*, 1991]. Estimates from the two hydraulic tests also agree with K estimates derived from grain-size analyses of core samples.

[26] One should note that these values represent horizontal K. Both the CHIT and the slug test analysis assume isotropy in K. At the submeter scale of the tests, this seems to be a valid assumption [*Burger and Belitz*, 1997] and the vertical K is expected to be within the range of the estimated horizontal K values at this scale.

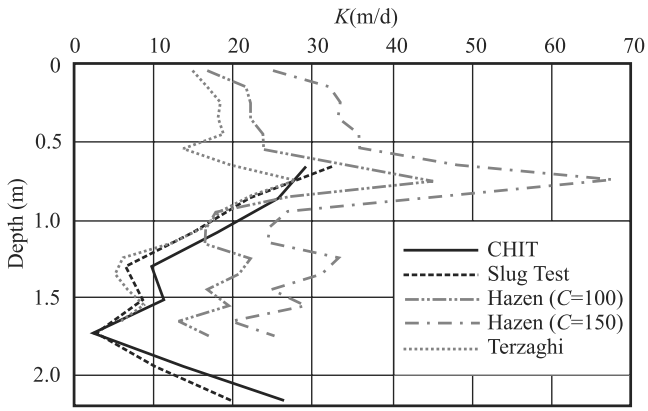

Figure 3. K estimates derived from different methods. Solid lines are estimates from hydraulic tests, and shaded lines are estimates from grain-size data.

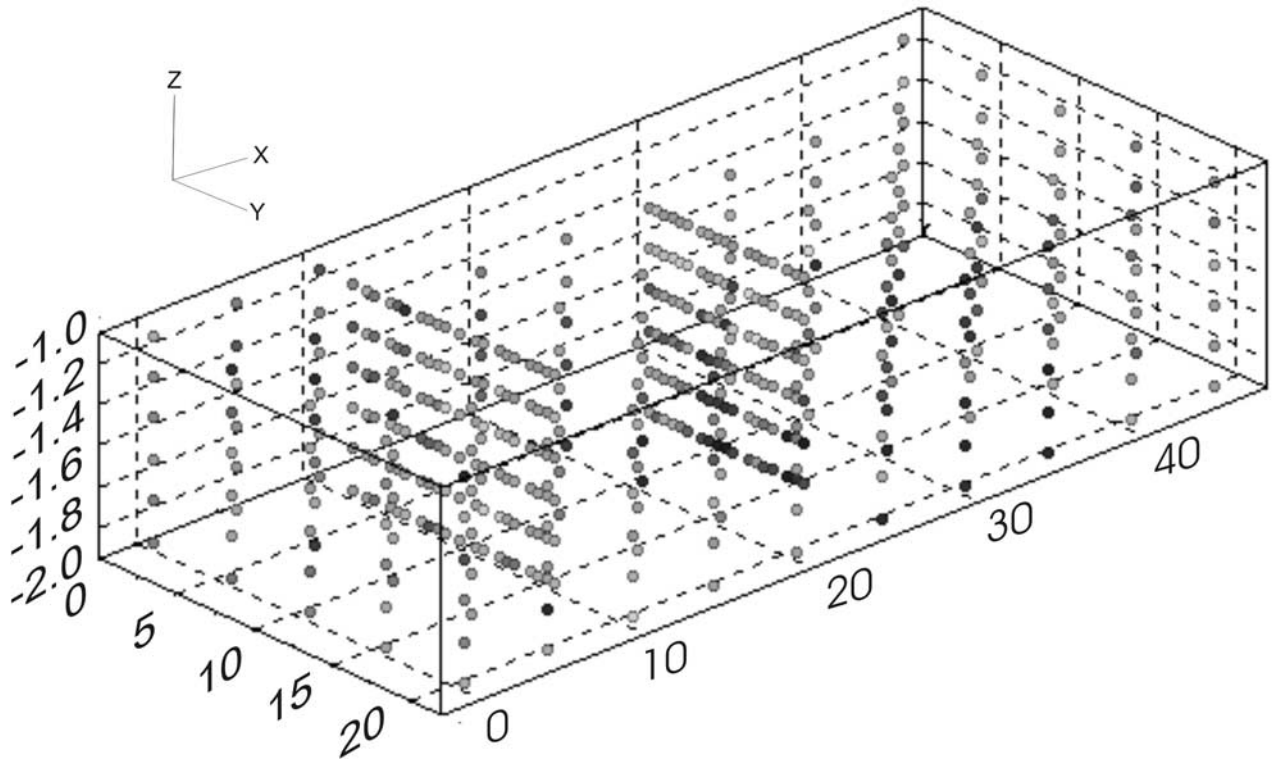

Figure 4. Location of K measurements in the volume of the Prairie Creek streambed. Top surface of grid is at 459.8 masl. Vertical exaggeration:10×. Axes are in meters.

[27] Preliminary experiments show that data from small-scale hydraulic tests are an effective proxy for broadly defined grain-size variations from one location to another. These techniques are thus promising tools for sedimentological mapping because they are devoid of problems associated with coring such as clogging of core barrel (rodding), poor recovery, and compaction resulting in inexact location of measurements, and disturbance of the deposits. We also show that the CHIT is a viable alternative for slug testing when doing tests in a streambed environment because of the abundance of and the proximity to water. In addition, data interpretation eliminates the need for curve-matching that is inherent in the analyses of slug tests. Hence this method is systematically used for estimating the 3D distribution of K.

[28] Measurements were conducted at six successive screen intervals, from a depth of 1 m to 2.2 m from a datum that is 460.8 masl. K was measured at 456 points in a 45 m × 20 m × 1.2 m block (total volume of 1080 m^3) of modern channel deposits (Figure 4). Sediments immediately below the streambed surface were not tested for K since these deposits are mobile even under typical low flow conditions. This also avoids having "flowing sands" when water is injected.

4.2. Geostatistical Analyses and Three-Dimensional Visualization

[29] Geostatistical analysis involved the determination of semivariograms $\gamma(h)$, or variograms, of K [*Gelhar*, 1993]:

$$\gamma(h) = \frac{1}{2N(h)} \sum_{|x_i - x_j| = h} \left[K(x_i) - K(x_j)\right]^2 \qquad (6)$$

where K is taken at position x_i and x_j that are separated by distance (lag) h. We use K instead of $\ln K$ because the K data is normally distributed (see section 5.1).

[30] Directional variograms were utilized for by-layer analysis of K. Directional variograms are variograms confined to a specified search direction, as compared to omnidirectional variograms that take into account all possible pairs. Transverse directional variograms were generated for each of the six measurement intervals. In addition, variograms in the vertical direction were generated from the four closely spaced cores. Exponential models, with no nuggets, were fit to the experimental variograms through nonlinear regression in all cases.

[31] The 3D K field was generated through application of the 3D kriging module of Mining Visualization System (MVS). The program automatically fits a spherical variogram model to the field data. This variogram is isotropic in the horizontal direction; anisotropy ratio of 10 was assigned to the vertical direction. The same package was used for visualization.

4.3. Global Estimation of Hydraulic Conductivity

[32] In hydrogeologic models, it is common to characterize the entire streambed by a single lumped parameter. This is referred to as "streambed conductance" [*Zlotnik et al.*, 1999; *Hunt et al.*, 2001; *Butler et al.*, 2001]. This parameter involves the "average" K and thickness of the streambed. The wide range of previously published K estimates [*Calver*, 2001] shows that the streambed is far from homogeneous as often assumed in hydrogeologic models.

[33] Using the data set of small-scale K and test locations, it is possible to upscale the data to a full tested volume. We used two techniques for estimation of effective hydraulic

conductivity of the streambed: simple volume averaging and 3D numerical Darcian experiments [*Warren and Price*, 1961]. The latter approach has been used extensively. For example, *Bierkens and Weerts* [1994] applied this approach to a synthetic K field that was generated for point bar deposits. Here, we use a real 3D data set with interpolation.

4.4. Ground-Penetrating Radar (GPR) Surveys

[34] Several GPR transects were conducted at the study site. *Davis and Annan* [1989] described the theory of GPR in applications to shallow subsurface investigations. We used integrated transmitting and receiving radars for two GPR surveying setups.

[35] In the first setup designed for normal streamflow conditions in June 2001, 400-Mhz and 100-Mhz center-frequency antennas were placed on an inflatable raft. The raft was floated along wooden tracks that allowed us to use an odometer wheel for distance measurements. Unfortunately, profiles from these surveys exhibited multiples of the water-sediment interface that obliterated most of the data which is a common problem [*Placzek and Haeni*, 1995; *Olimpio*, 2000]. This situation may require unconventional methods of surveying [*Meyers and Smith*, 1997].

[36] In the second setup, a 250-Mhz center frequency cart-mounted antenna was used in almost dry conditions in September 2001. In both surveys (June and September), the radar units continuously collected traces as they were moved along the transect lines, similar to a common offset gather in seismic reflection.

[37] Processing of the GPR data was kept to a minimum. Automatic gain control, signal saturation correction ("dewow"), and depth migration were implemented using Win_EKKO_Pro [*Sensors and Software, Inc.*, 2001]. The propagation velocities of the electromagnetic waves through the streambed were estimated using an automated hyperbola matching method.

4.5. Comparison to Meander Bend Deposits

[38] After a 3D image of K distribution was generated, we visually compared it to sedimentological observations in similar channel bend environments [*Bridge*, 1977]. This allowed us to correlate the mapped portion of the streambed to a process known to occur in the studied bend.

[39] Scouring predominates in a channel bend. Thus we use the GPR profiles to identify and locate possible scour surfaces. We also compare the K data to the geophysical data for consistency.

5. Results and Discussion

5.1. Local K Estimates

[40] CHIT was used to gather the extensive K data set of the modern streambed. The K values of the streambed ranged from 0.15 m/d to 74.7 m/d. The summary statistics are in Table 1. *Calver* [2001] presented a streambed K range of 0.001 m/d to 100 m/d based on 41 different references. The K range encountered within the investigated small portion of the Prairie Creek's streambed is consistent with *Calver*'s [2001] observations.

Table 1. Summary Statistics of CHIT Results

Data Type/Statistic	K, m/d	ln$K$
Number of samples	456	456
Mean	22.3	2.84
Maximum	74.7	4.31
Minimum	0.1	−1.92
Standard deviation	13.3	0.86
Kolmogorov-Smirnov D	0.06	0.55

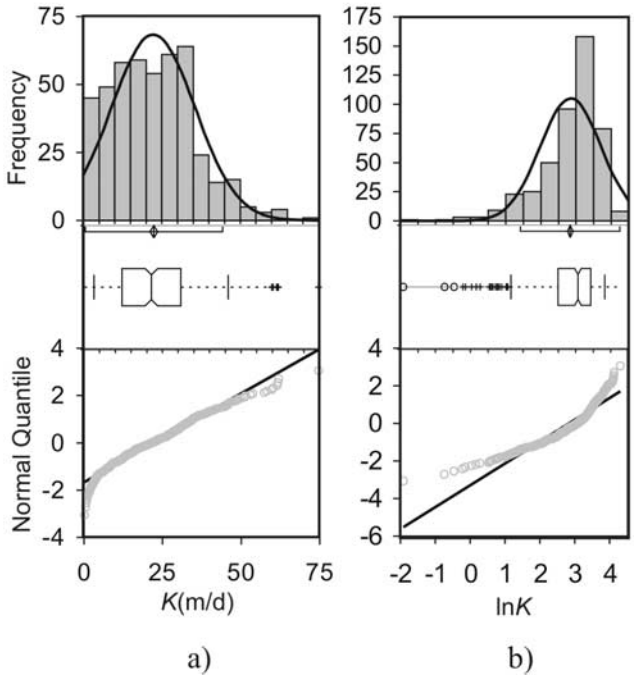

Figure 5. Histograms, boxplots, and normal quantile plots of (a) K data and (b) ln-K data. Top charts depict normal distribution curves fitted to the actual histograms; middle charts show the 5th, 25th, 50th, 75th and 95th quantiles as well as outliers (open circles and crosses); bottom charts compare the actual quantiles (open circles) to expected normal quantiles (line).

[41] Kolmogorov-Smirnov tests show that the K data are normally distributed [*Sprent*, 1993]. This is exemplified by the histograms (Figure 5). Deviation of our results from commonly observed lognormal distributions for K are best explained by the fact that only channel deposits were analyzed. If other facies, such as overbank deposits, were also considered a lognormal distribution for K would be likely.

5.2. Effective Hydraulic Conductivity of Streambed

[42] The effective hydraulic conductivity was obtained through procedures outlined in section 4.3. For upscaling of the 456 measured points in a 1080 m^3 block, a 3D K field was generated through ordinary kriging using MVS.

[43] In simple volume averaging, the domain was subdivided into volumes bounded by isosurfaces (analogous to contaminant plumes bounded by concentration limits). The isosurfaces correspond to K intervals of 5 m/d. The midpoint of each interval was used as the value for that interval in the averaging process. The volume of each interval was determined using the "volume and mass" module of MVS. The K estimates were upscaled through

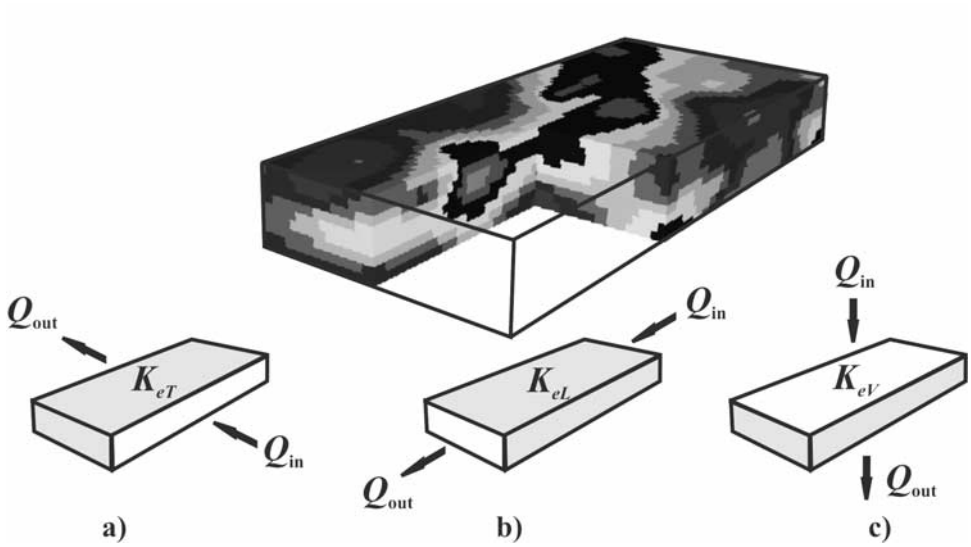

Figure 6. MODFLOW models used for calculating effective K in different directions. Gray-shaded boundaries are no-flow boundaries, clear faces are constant-head boundaries. (a) K_{eT} = 18.5 m/d - transverse case, (b) K_{eL} = 19.5 m/d - longitudinal case, and (c) K_{eV} = 18.1 m/d - vertical case. See color version of this figure at back of this issue.

computation of the arithmetic mean K_A and geometric mean K_G:

$$K_A = \frac{1}{V_T}\sum_{i=1}^{n} V_i K_i, \qquad \ln K_G = \frac{1}{V_T}\sum_{i=1}^{n} V_i \ln K_i, \qquad V_T = \sum_{i=1}^{n} V_i \tag{7}$$

where n is number of K intervals, K_i and V_i are the K and volume of the block associated with i-th interval respectively, and V_T is the total averaging volume. Simple volume averaging results in arithmetic mean K_A = 17.9 m/d and geometric mean K_G = 15.4 m/d.

[44] In upscaling that utilizes 3D numerical simulations, we followed the *Warren and Price* [1961] approach. The K data was used in numerical flow simulation in the finite difference code MODFLOW [*McDonald and Harbaugh*, 1984]. The 3D K field was discretized into 0.5 m × 0.5 m × 0.13 m blocks. Of the six sides of the domain, four were assigned as no-flow boundaries. The remaining two opposing faces were assigned as constant-head boundaries (Figure 6). Three orthogonal flow directions were imple-

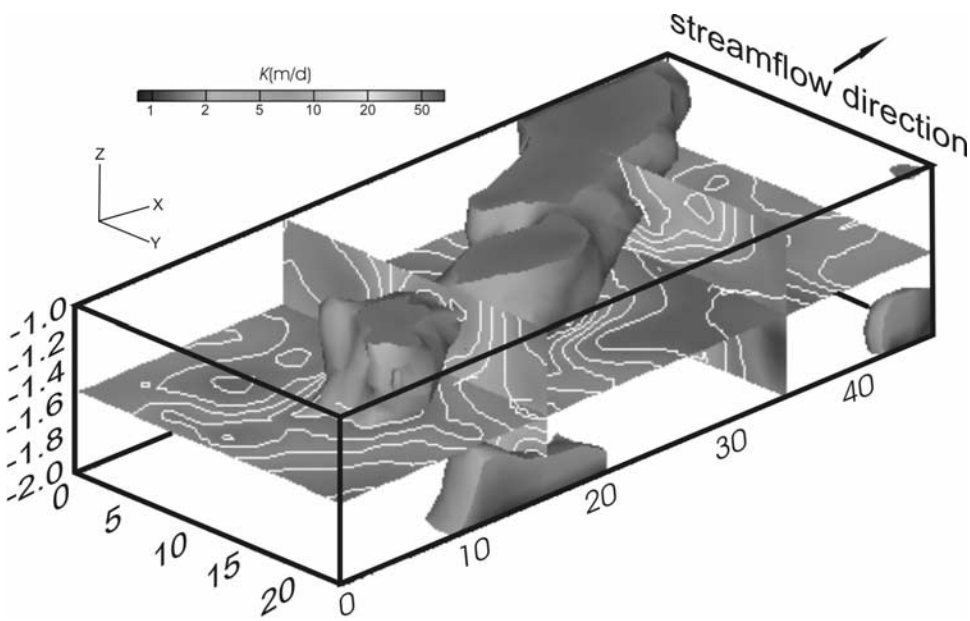

Figure 7. Three-dimensional hydraulic conductivity field generated through kriging of K. Shaded arcuate region corresponds to K of ≥30 m/d. Note vertical exaggeration:10× and that inset color legend is logarithmic. K isoline interval on sections is 5 m/d. Axes are in meters. See color version of this figure at back of this issue.

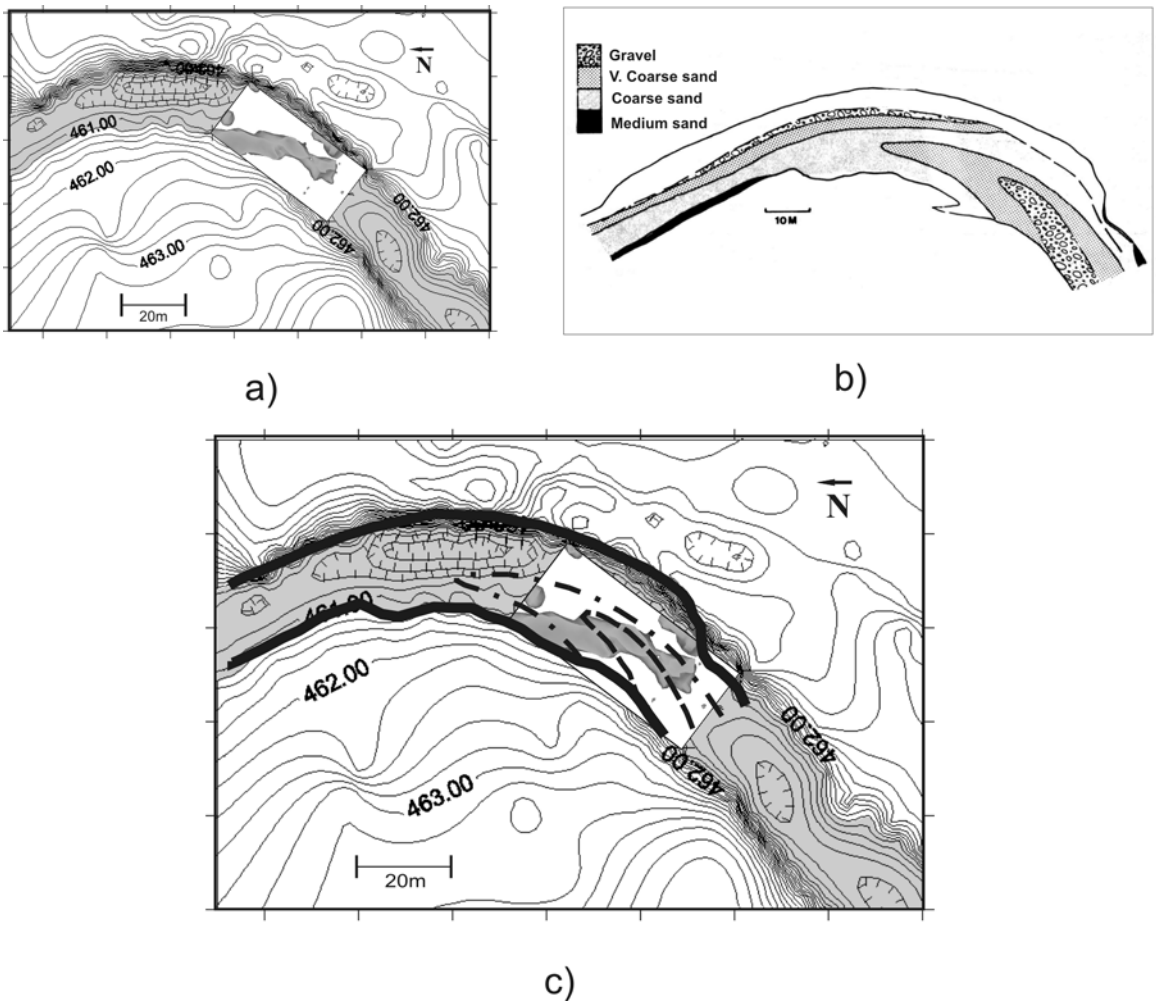

Figure 8. Comparison of channel bend deposits: (a) Prairie Creek data based on CHIT; (b) channel bend deposits as observed on River South Esk, Scotland (modified from *Bridge* [1977], reprinted with permission of John Wiley); (c) is a superposition of Figures 8a and 8b. Solid lines represent the river banks, dashed-dotted lines bound very coarse sand deposits, and dashed lines bound gravel deposits.

mented through redistribution of the boundaries: two components in the horizontal direction, and one in the vertical direction. The resulting discharge is then used in Darcy's Law to estimate the effective longitudinal hydraulic conductivity K_{eL}, transverse horizontal hydraulic conductivity K_{eT}, and vertical hydraulic conductivity K_{eV}. Numerical Darcian experiments yield effective values K_{eT} = 18.5 m/d, K_{eL} = 19.5 m/d, and K_{eV} = 18.1 m/d. Corresponding values of mass balance errors of 0.002%, 0.6% and 0.0003% for the transverse, longitudinal and vertical numerical models are within the acceptable range.

[45] Two observations are apparent from the upscaling experiments. First, numerically modeled upscaled parameters agree with the results from volumetric averaging. Second, ''global'' estimates of K exhibit horizontal and vertical isotropy. *Bierkens and Weerts* [1994] found that cross bedding and core scale anisotropy has an impact on numerically upscaled K tensor of point bar deposits. Unfortunately, the in situ small-scale hydraulic techniques that we used do not yield local K anisotropy as any single-borehole technique (see discussion by *Zlotnik et al.* [2001]). This hinders verification of core scale anisotropy effects on effective K values of the streambed.

5.3. Three-Dimensional Spatial Structure of Modern Streambed Deposits

[46] A shaded arcuate channel-like feature is portrayed in Figure 7. This shaded region has a K of $\geq$30 m/d. The 3D representation of the K data set of the tested streambed deposits allows us to infer the extent of the modern streambed. It is tempting to interpret this feature as a main channel deposit simply owing to its elongated geometry. We go a step further by comparing this to surface channel-bend deposits.

[47] Sedimentologic investigations show that river bend deposits are laid in a predictable manner when bank-full or near-bank-full conditions are met [*Parker and Andrews*, 1985; *Bridge*, 1992]. We overlay a 2D top view of the shaded high-K region with observations presented by *Bridge* [1977] on the meandering River South Esk in Scotland (Figure 8c). The bend at our site and the studied bend of the River South Esk have similar scale and shape.

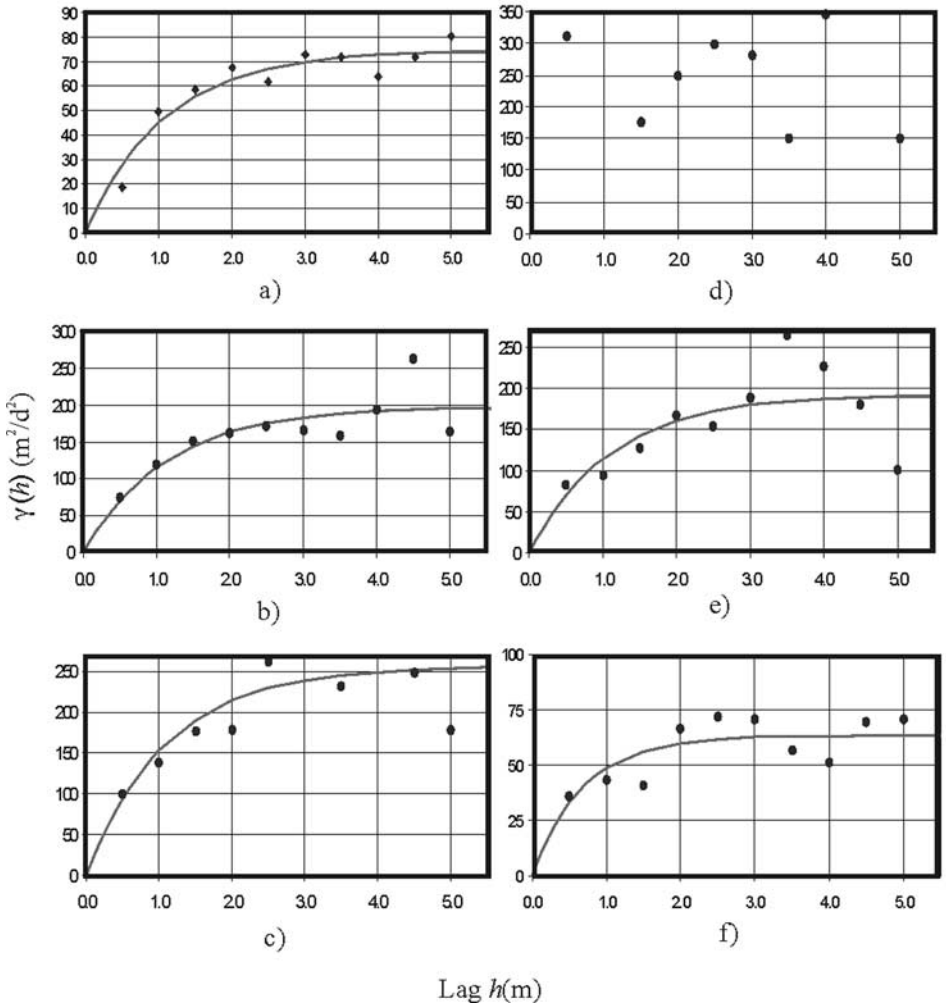

Figure 9. Transverse directional variograms and fitted exponential models for different depths: (a) 1.1 m; (b) 1.3 m; (c) 1.5 m; (d) 1.7 m (no variogram model was fit here due to poor definition of spatial structure); (e) 1.9 m; (f) 2.1 m.

[48] The shaded high-K area coincides with the location where coarser grained deposits were observed on the River South Esk. Minor discrepancies are due to lateral translation of the channel and possibly vertical aggradation or incision. Thus the sediments close to the surface in our study site are related to the modern bend-flow regime of the stream. Deeper sediments lose this pattern and thus were deposited in a different regime. This trend is also exemplified by

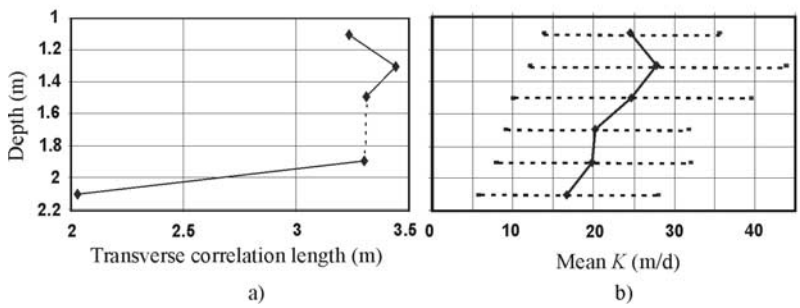

Figure 10. Statistical properties of K at various depths: (a) transverse correlation length, (b) mean K at each depth interval (with one standard deviation). No transverse correlation length was determined for the interval at 1.6 m–1.8 m due to poor definition of spatial structure (see Figure 9d).

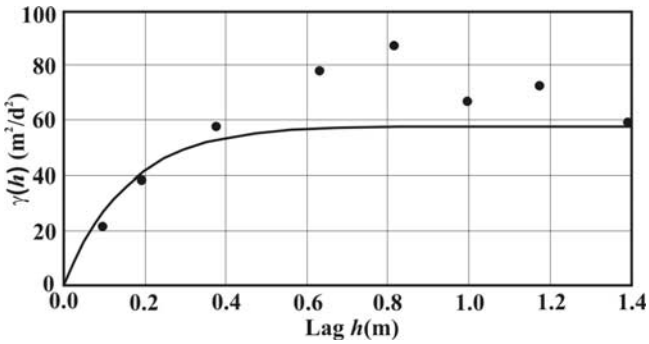

Figure 11. Vertical variogram based on core samples (see location in Figure 1).

transverse directional variograms taken at each depth interval (Figure 9). At a depth of >2 m from the top of the grid, the lateral structure of the tested media changes drastically. This change is further depicted in Figure 10a where the abrupt change in spatial structure (correlation scale in transverse direction) at the same depth interval occurs. This is best explained by a change in depositional regime associated with the deposits. Notably, the statistical distribution of K data for each depth interval tends to stay constant (Figure 10b).

[49] The vertical directional variogram based on the core data agrees well with the observed change of structure through depth (Figure 11). A vertical correlation scale of 0.53 m is consistent with observations in similar environments [*Davis et al.*, 1997].

5.4. GPR Profiles

[50] We conducted a second GPR survey in September 2001 when the Prairie Creek was nearly dry, this time using a radar unit mounted on a cart. Two processed transverse GPR sections (A-A′ and B-B′) display a relatively continuous reflector that dips toward the cutbank (Figure 12). These two parallel profiles are about a 1.5 m apart. We interpret this reflector to be a major scour surface formed during a flood. It can also be observed that the reflectors above this surface are more closely spaced than the reflectors beneath it. The shallow concave reflectors are suggestive of trough cross bedding.

[51] Superposition of K isolines from a cross section from the kriged 3D K field to a GPR profile from the same location (B-B′) does not show perfect correspondence between the two data sets (Figure 13). Nonetheless, the isolines corresponding to K of 10, 15, and 20 m/d tend to mimic the inclined reflectors below the aforementioned major scour surface. The location of the high K region on top view also corresponds to the location of coarser grained deposits within the similar channel bend of the River South Esk (Figures 7 and 8). Thus the deeper inclined reflector/scour surface and the high-K region were likely formed by the same or similar flood events. This high-K area is a 3D manifestation of floods as they wane and deposit sediments. The extent of the dipping reflector or major scour surface

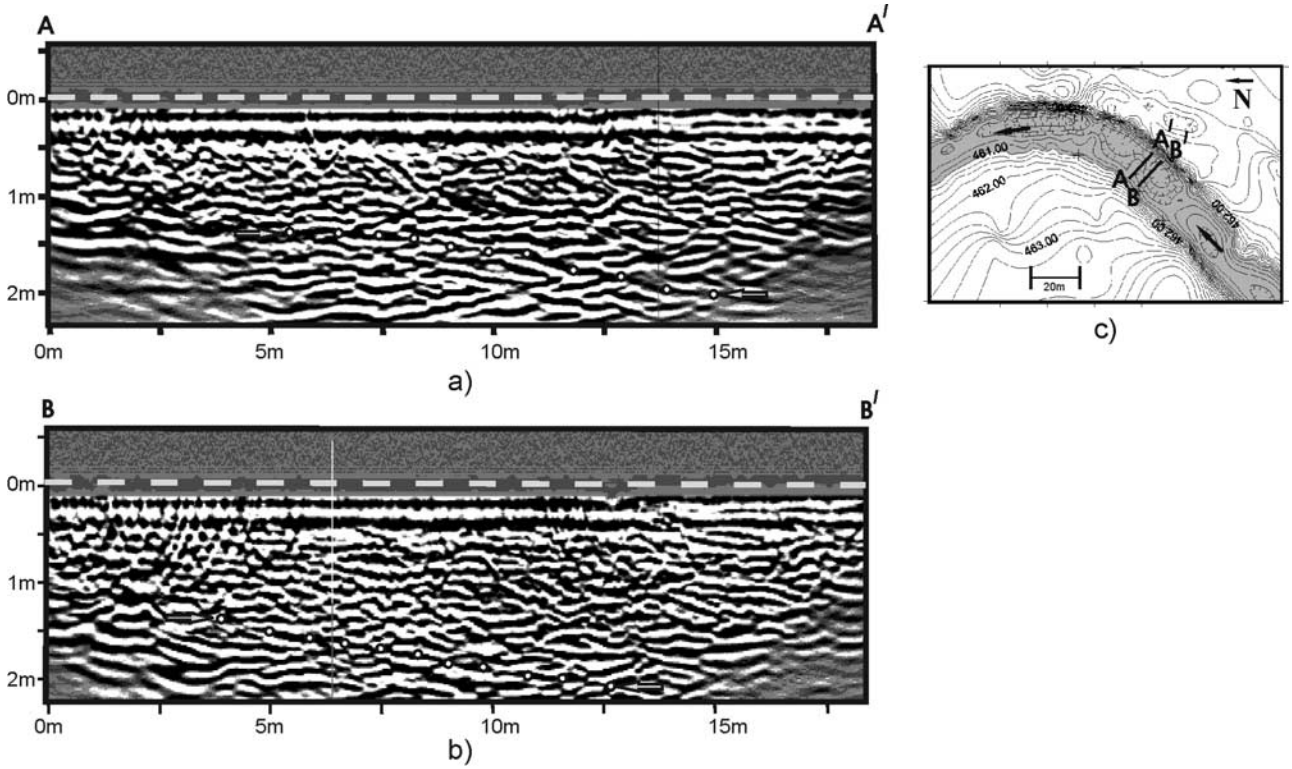

Figure 12. GPR profiles across the Prairie Creek 1.5 m apart: (a) downstream section A-A′; (b) upstream section B-B′; (c) location of GPR profiles. Arrows in Figures 12a and 12b point to ends of semicontinuous reflector (traced by a series of open circles) interpreted as a major scour surface dipping toward the direction of the cutbank.

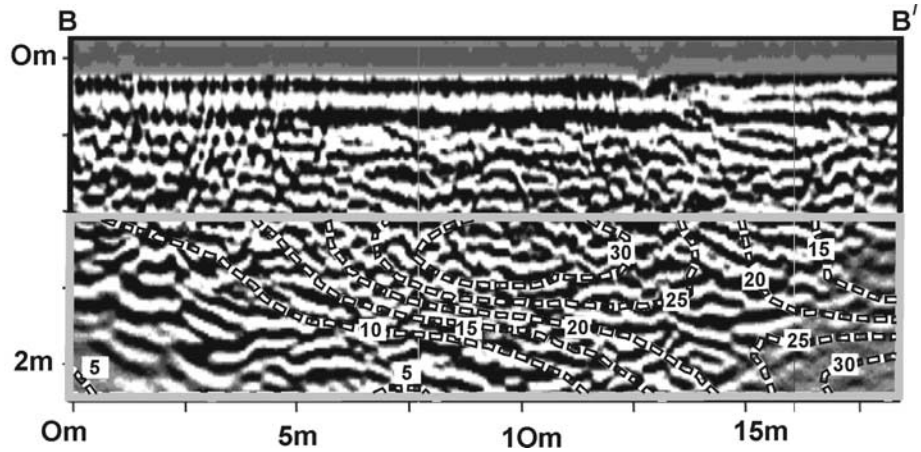

Figure 13. Superposition of GPR profile B-B′ and corresponding *K* cross section. *K* isolines are in m/d. Profile B-B′ location is shown in Figure 12c.

can be then used to limit the extent of the streambed. In our case, this depth is about 2 m from the top of the grid.

[52] The agreement between the deep inclined reflectors with the shape and location of the 10 m/d, 15 m/d, and 20 m/d isolines adds confidence in the kriging procedure used (MVS utilized sill and correlation scales ten times smaller in the vertical direction than in the horizontal direction). Incorporation of horizontal anisotropy produced an elongate high-*K* region similar to what was presented, although the surface bounding this volume was more irregular. Smaller high-*K* lenses were also generated in this case. However, consideration of previous sedimentologic studies, in addition to the GPR data, leads us to accept the present methodology and 3D realization of *K*.

6. Summary

[53] Small-scale hydraulic testing permitted accurate 3D mapping of unconsolidated sediments since it overcomes common problems associated with coring such as sample disturbance, poor recovery, compaction, and rodding that limit accurate sample location. We first compared methods for mapping *K* fields of modern streambed substrates or the 'hyporheic zone'. Small-scale constant-head injection tests appear to give results with accuracy that is comparable to information from grain-size analysis of core samples. The range of *K* values (0.1 m/d to 74.7 m/d) based on CHIT almost covers the entire range of published values [*Calver*, 2001]. It is apparent that this wide range can be attributed to site-specific heterogeneity (such as the case here) and this strongly supports the need for detailed field tests when considering streambed deposits in hydrogeologic models.

[54] Estimation of the effective *K* of the volume gives the consistent values of arithmetic mean (K_A = 17.9 m/d), geometric mean (K_G = 15.4 m/d), and effective *K* in transverse, longitudinal, and vertical directions (K_{eT} = 18.5 m/d, K_{eL} = 19.5 m/d, and K_{eV} = 18.1 m/d). These values are well within the range presented by *Calver* [2001]. Presented here is a unique case where numerous 3D field measurements are lumped into effective values.

[55] Structure-imitating interpolation (kriging) of our extensive data set resulted in a realization that is consistent with surficial observations of grain-size distributions in a similar modern environment. This not only supports the plausibility of our generalization of the streambed but also links our tested domain to well-studied modern processes. Furthermore, this permits us to interpret our results in a process-oriented framework.

[56] The agreement between the 3D structure of deposits at our site and the published observations support the conclusion that the substrate was formed in a regime similar to that of the meandering River South Esk. The loss of this observed pattern with depth constrains the depth/thickness of these deposits. This is further supported by the changing nature of directional variograms with depth and the presence of scour surfaces in GPR profiles.

[57] This study shows that the representation of the streambed as an entity of constant width, thickness, and hydraulic properties is a simplified generalization of actual streambed properties. This oversimplification has important ramifications to groundwater-surface water interaction studies. Thus the streambed can only be better understood and more realistically represented in models if the spatial variability of its hydraulic properties, as well as its geometry, is investigated in further detail. Several studies attempted to address this issue through simulation of synthetic fluvial deposits. We present a case where a modern streambed is investigated in three dimensions through integration of techniques from hydrogeology, geophysics and geostatistics and concepts from sedimentology.

[58] **Acknowledgments.** This research was supported by USGS Grant 1434HQ96GR02683 and grants from the Central Platte Natural Resources District (CPNRD) (1999–2002). M. Bayani Cardenas received student grants from the AAPG Grants-in-Aid Foundation (Paul Danheim Nelson Named Grant), AAPG Mid-Continent Section, and Nebraska-Geological Society (Yatkola-Edwards Research Grant). The University of Nebraska-Lincoln (UNL) Water Center supported the acquisition of GPR unit. The UNL Department of Geosciences provided summer fellowships and logistical support. The authors thank Stefan J. Kollet of UNL, Department of Geosciences, for fruitful discussions, and Reed Copsey of CTECH Development Corporation who graciously provided access to MVS. The help of Justin Jakub and Ram Narayanan of UNL, Electrical Engineering, and of CPNRD staff in the GPR data acquisition is greatly appreciated. Initial drafts of this manuscript were vastly improved after helpful comments from Norman D. Smith of UNL, and reviews from Whitney J. Autin and an anonymous reviewer.

References

Bencala, K. E., A perspective on stream-catchment connections, *J. N. Am. Benthol. Soc.*, *12*(1), 44–47, 1993.

Bierkens, M. F. P., and H. J. T. Weerts, Block hydraulic conductivity of cross-bedded fluvial sediments, *Water Resour. Res.*, *30*(10), 2665–2678, 1994.

Bouwer, H., and R. C. Rice, A slug test for determining hydraulic conductivity of unconfined aquifers with completely or partially penetrating wells, *Water Resour. Res.*, *12*(3), 423–428, 1976.

Bridge, J. S., Flow, bed topography, grain size and sedimentary structure in open channel bends: A three-dimensional model, *Earth Surf. Processes*, *2*, 401–416, 1977.

Bridge, J. S., A revised model for water flow, sediment transport, bed topography, and grain size sorting in natural river bends, *Water Resour. Res.*, *28*(4), 999–1013, 1992.

Butler, J. J., Jr., *The Design, Performance, and Analysis of Slug Tests*, 252 pp., A. F. Lewis, New York, 1998.

Butler, J. J., Jr., V. A. Zlotnik, and M.-S. Tsou, Drawdown and stream depletion produced by pumping in the vicinity of a partially penetrating stream, *Ground Water*, *39*(5), 651–659, 2001.

Burger, R. L., and K. Belitz, Measurement of anisotropic hydraulic conductivity in unconsolidated sands: A case study from a shoreface deposit, Oyster, Virginia, *Water Resour. Res.*, *3*(6), 1515–1522, 1997.

Calver, A., Riverbed permeabilities: Information from pooled data, *Ground Water*, *39*(4), 546–553, 2001.

Davis, J. L., and A. P. Annan, Ground penetrating radar for high-resolution mapping of soil and rock stratigraphy, *Geophys. Prospect.*, *37*, 531–551, 1989.

Davis, J. M., J. L. Wilson, F. M. Phillips, and M. B. Gotkowitz, Relationship between fluvial bounding surfaces and the permeability correlation structure, *Water Resour. Res.*, *33*(8), 1843–1854, 1997.

Dowdy, S., and S. Wearden, *Statistics for Research*, 629 pp., John Wiley, New York, 1991.

Duwelius, R. F., Hydraulic conductivity of the streambed, east branch Grand Calumet River, northern Lake County, Indiana, *U.S. Geol. Surv. Water Resour. Invest. Rep.*, *96-4218*, 37 pp., 1996.

Gelhar, L. W., *Stochastic Subsurface Hydrology*, 390 pp., Prentice-Hall, Old Tappan, N. J., 1993.

Gelhar, L. W., C. Welty, and K. R. Rehfeldt, A critical review of data on field-scale dispersion in aquifers, *Water Resour. Res.*, *28*(7), 1955–1974, 1992.

Harvey, J. W., B. J. Wagner, and K. E. Bencala, Evaluating the reliability of the stream tracer approach to characterize stream-subsurface water exchange, *Water Resour. Res.*, *32*(8), 2441–2451, 1996.

Hinsby, K., P. L. Bjerg, L. J. Andersen, B. Skov, and E. V. Clausen, A mini slug test method for determination of a local hydraulic conductivity of an unconfined sandy aquifer, *J. Hydrol.*, *136*, 87–106, 1992.

Hunt, B., J. Weir, and B. Clente, A stream depletion field experiment, *Ground Water*, *39*(2), 283–289, 2001.

Kollet, S. J., and V. A. Zlotnik, Stream depletion predictions using pumping test data from a heterogeneous stream-aquifer system (A case study from the great plains, USA), *J. Hydrology*, in press, 2003.

Koltermann, C. E., and S. M. Gorelick, Heterogeneity in sedimentary deposits: A review of structure-imitating, process-imitating, and descriptive approaches, *Water Resour. Res.*, *32*(9), 2617–2658, 1996.

Landon, M. K., D. L. Rus, and F. E. Harvey, Comparison of instream methods for measuring hydraulic conductivity in sandy streambeds, *Ground Water*, *39*(6), 870–885, 2001.

McDonald, M. G., and A. W. Harbaugh, A modular three-dimensional finite-difference groundwater flow model, *U.S. Geol. Surv. Open File Rep.*, *83*, 875 pp., 1984.

Meyers, R. A., and D. G. Smith, Submersible ground penetrating radar a new geophysical tool to assess channel-fills, scours and sub-fill bedrock topography, *Geol. Soc. Am. Abstr. Programs*, *29*(6), 448, 1997.

Olimpio, J. R., Use of a ground-penetrating radar system to detect pre- and post-flood scour at selected bridge sites in New Hampshire, 1996–98, *U.S. Geol. Surv. Water Resour. Invest. Rep.*, *00-4035*, 28 pp., 2000.

Palmer, M. A., Experimentation in the hyporheic zone: Challenges and prospectus, *J. N. Am. Benthol. Soc.*, *12*(1), 84–93, 1993.

Parker, G., and E. D. Andrews, Sorting of bed load sediment by flow in meander bends, *Water Resour. Res.*, *21*(9), 1361–1373, 1985.

Placzek, G., and F. P. Haeni, Surface-geophysical techniques used to detect existing and infilled scour holes near bridge piers, *U.S. Geol. Surv. Water Resour. Invest. Rep.*, *95-4009*, 44 pp., 1995.

Rus, D. L., V. L. McGuire, B. R. Zurbuchen, and V. A. Zlotnik, Vertical profiles of streambed hydraulic conductivity determined using slug tests in central and western Nebraska, *U.S. Geol. Surv. Water Resour. Invest. Rep.*, *01-4212*, 32 pp., 2001.

Scheibe, T. D., and D. L. Freyberg, The use of sedimentological information for geometric simulation of natural porous media structure, *Water Resour. Res.*, *31*(12), 3259–3270, 1995.

Sensors and Software, Inc., Win_EKKO user's guide version 1.0, *Tech. Manual 30*, 68 pp., Ontario, Canada, 2001.

Sniegocki, R. T., Ground-water resources of the Prairie Creek unit of the lower Platte River basin, Nebraska, *U.S. Geol. Surv. Water Supply Pap. 1327*, 133 pp., 1955.

Sophocleous, M. A., A. D. Koussis, J. L. Martin, and S. P. Perkins, Evaluation of simplified stream-aquifer depletion models for water rights administration, *Ground Water*, *33*(4), 579–588, 1995.

Sprent, P., *Applied Nonparametric Statistical Methods*, 2nd ed., 342 pp., Chapman and Hall, New York, 1993.

Springer, A. E., W. D. Petroutson, and B. A. Semmens, Spatial and temporal variability of hydraulic conductivity in active reattachment bars of the Colorado River, Grand Canyon, *Ground Water*, *37*(3), 338–344, 1999.

Sun, T., P. Meakin, and T. Jøssang, A computer model for meandering rivers with multiple bed load sediment sizes: 2. Computer simulations, *Water Resour. Res.*, *37*(8), 2243–2258, 2001.

Vukovic, M., and A. Soro, *Determination of Hydraulic Conductivity of Porous Media From Grain-Size Composition*, 83 pp., Water Resour. Publ., Highlands Ranch, Colo., 1992.

Warren, J. E., and H. S. Price, Flow in heterogeneous porous media, *Soc. Pet. Eng. J.*, *1*, 153–169, 1961.

Webb, E. K., and M. P. Anderson, Simulation of preferential flow in three-dimensional, heterogeneous conductivity fields with realistic internal architecture, *Water Resour. Res.*, *32*(3), 533–545, 1996.

Webb, E. K., and J. M. Davis, Simulation of the spatial heterogeneity of geologic properties: An overview, in *Hydrogeologic Models of Sedimentary Aquifers*, edited by G. S. Fraser and J. M. Davis, pp. 1–24, Soc. for Sediment. Geol., Tulsa, Okla., 1998.

Woessner, W. W., Stream and fluvial plain ground water interactions: Rescaling hydrogeologic thought, *Ground Water*, *38*(3), 423–429, 2000.

Zlotnik, V., Interpretation of slug and packer tests in anisotropic aquifers, *Ground Water*, *32*(5), 761–766, 1994.

Zlotnik, V. A., and H. Huang, Effect of partial penetration and streambed sediments on aquifer response to stream stage fluctuations, *Ground Water*, *37*(4), 599–605, 1999.

Zlotnik, V. A., and V. L. McGuire, Multi-level slug tests in highly permeable formations: 2. Hydraulic conductivity identification, method verification, and field applications, *J. Hydrol.*, *204*, 283–296, 1998.

Zlotnik, V., H. Huang, and J. J. Butler Jr., Evaluation of stream depletion considering finite stream width, shallow penetration, and properties of streambed sediments, in *Proceedings of Joint Congress, Water 99, Brisbane, Australia, July 6-8*, pp. 221–226, Inst. of Eng. Aust., Brisbane, 1999.

Zlotnik, V. A., B. R. Zurbuchen, and T. Ptak, The steady-state dipole-flow test for characterization of hydraulic conductivity statistics in a highly permeable aquifer; Horkheimer Insel site, Germany, *Ground Water*, *39*(4), 504–516, 2001.

Zurbuchen, B. R., V. A. Zlotnik, and J. J. Butler Jr., Dynamic interpretation of slug tests in highly permeable aquifers, *Water Resour. Res.*, *38*(3), 1025, doi:10.1029/2001WR000354, 2002.

M. B. Cardenas, Department of Earth and Environmental Science, New Mexico Institute of Mining and Technology, Socorro, New Mexico 87801, USA. (cardenas@nmt.edu)

V. A. Zlotnik, Department of Geosciences, University of Nebraska at Lincoln, Lincoln, NE 68588, USA.

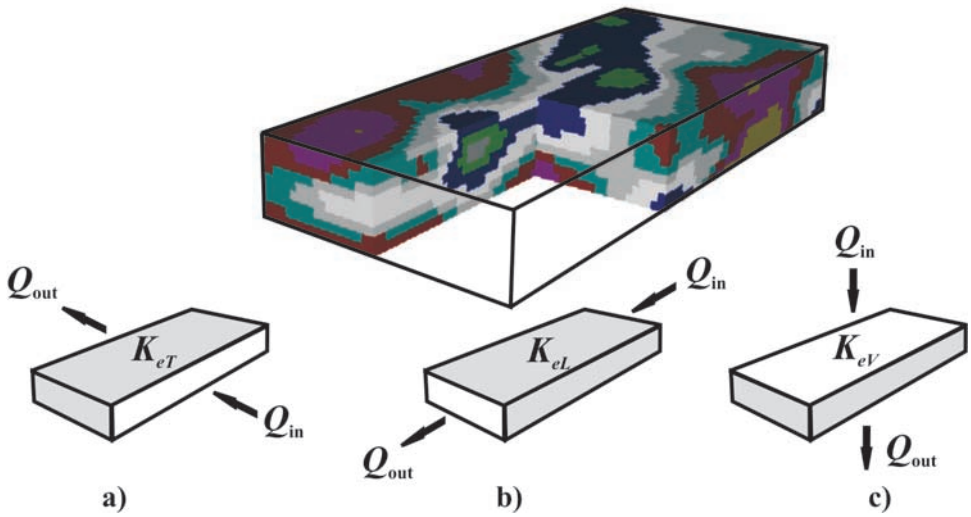

Figure 6. MODFLOW models used for calculating effective K in different directions. Gray-shaded boundaries are no-flow boundaries, clear faces are constant-head boundaries. (a) K_{eT} = 18.5 m/d - transverse case, (b) K_{eL} = 19.5 m/d - longitudinal case, and (c) K_{eV} = 18.1 m/d - vertical case.

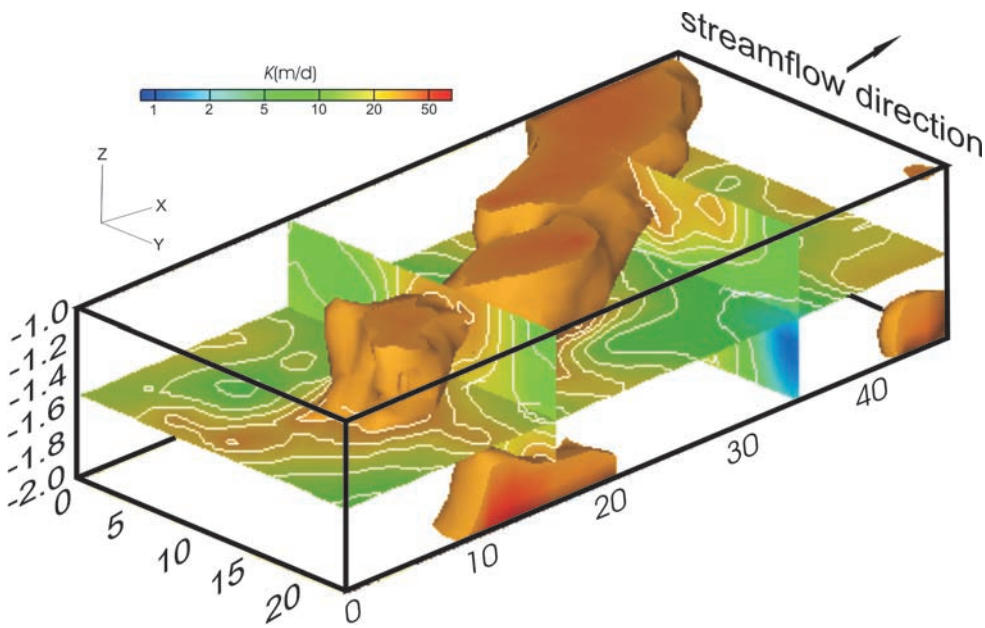

Figure 7. Three-dimensional hydraulic conductivity field generated through kriging of K. Shaded arcuate region corresponds to K of $\geq$30 m/d. Note vertical exaggeration:10$\times$ and that inset color legend is logarithmic. K isoline interval on sections is 5 m/d. Axes are in meters.